Changes in sediment methanogenic archaea community structure and methane production potential following conversion of coastal marsh to aquaculture ponds

Ping Yang[a,b,c*], Kam W. Tang[d], Chuan Tong[a,b,c], Derrick Y. F. Lai[e], Lianzuan Wu[b], Hong Yang[f,g], Linhai Zhang[a,b,c], Chen Tang[b], Yan Hong[b], Guanghui Zhao[b]

[a]*School of Geographical Sciences, Fujian Normal University, Fuzhou 350007, P.R. China*

[b]*Key Laboratory of Humid Subtropical Eco-geographical Process of Ministry of Education, Fujian Normal University, Fuzhou 350007, P.R. China*

[c]*Research Centre of Wetlands in Subtropical Region, Fujian Normal University, Fuzhou 350007, P.R. China*

[d]*Department of Biosciences, Swansea University, Swansea SA2 8PP, U. K.*

[e]*Department of Geography and Resource Management, The Chinese University of Hong Kong, Hong Kong, China*

[f]*College of Environmental Science and Engineering, Fujian Normal University, Fuzhou, 350007, China*

[g]*Department of Geography and Environmental Science, University of Reading, Reading, UK*

***Correspondence to:** Ping Yang (yangping528@sina.cn)

Telephone: 086-0591-87445659 **Fax:** 086-0591-83465397

A B S T R A C T

Widespread conversion of coastal wetlands into aquaculture ponds in the Chinese coastal region often results in degradation of the wetland ecosystems, but its effects on sediment's potential to produce greenhouse gases remain unclear. Using field sampling, incubation experiments and molecular analysis, we studied the sediment CH_4 production potential and the relevant microbial communities in a brackish marsh and the nearby aquaculture ponds in the Min River Estuary in southeastern China. Sediment CH_4 production potential was higher in the summer and autumn months than in spring and winter months, and it was best correlated with sediment carbon content among all environmental variables. The mean sediment CH_4 production potential in the aquaculture ponds (20.1 ng g^{-1} d^{-1}) was significantly lower than that in the marsh (45.2 ng g^{-1} d^{-1}). While *Methanobacterium* dominated in both habitats (41-59%), the overall composition of sediment methanogenic archaea communities differed significantly between the two habitats ($p<0.05$) and methanogenic archaea alpha diversity was lower in the aquaculture ponds ($p<0.01$). Network analysis revealed that interactions between sediment methanogenic archaea were much weaker in the ponds than in the marsh. Overall, these findings suggest that conversion of marsh land to aquaculture ponds significantly altered the sediment methanogenic archaea community structure and diversity and lowered the sediment's capacity to produce CH_4.

Keywords: Methane production; Methanogenic archaea; Network analysis; Land-use and land coverage change (LULCC); Coastal wetlands; Aquaculture systems

1. Introduction

Methane (CH_4) has a 45-times higher mass-specific global warming potential than carbon dioxide (CO_2) over a 100-year period (Neubauer and Megonigal, 2015), and it contributes to approximately 20% of the global radiative forcing (IPCC, 2013). The average atmospheric CH_4 concentration reached 1875 ppbv in 2019 (National Oceanic and Atmospheric Administration, 2020), exceeding the pre-industrial levels by about 150%. Aquatic CH_4 is primarily produced in sediments by methanogenic archaea during the terminal step of organic diagenesis under anaerobic conditions (Gruca-Rokosz et al., 2020; Lai, 2009; Lofton et al., 2015; Liu et al., 2019). Land use and land cover change (LULCC) can lead to changes in hydrology, nutrient cycles, sediment properties and overall ecosystem functions (Andreetta et al., 2016; Dick and Osunkoya, 2000; Liu et al., 2021), and has been shown to be a major driver of anthropogenic CH_4 emissions in terrestrial and aquatic ecosystems (Chen et al., 2021; IPCC, 2013; Reay et al., 2018; Tan et al., 2020).

Coastal wetlands, located at the interface between the terrestrial and marine environments, are sites of intense biological production (Chmura et al., 2003; Han et al., 2014; Doroski et al., 2019). LULCC has increasing impacts on coastal wetlands (Hao et al., 2020; Liu and Mo, 2016) and has already caused degradation or loss of about 50% of the world's coastal wetlands (Barbier et al., 2011). China (Sun et al., 2015) and the wider Asia-Pacific region (Romañach et al., 2018) are experiencing among the worst wetland degradation due to continuous population and economic growth, rapid urbanization and infrastructure development. It is estimated that 27% of the available wetland area in the Asia has been drained or converted to farmland for intensive food production (Huang et al., 2010), and the conversion of coastal wetlands to aquaculture ponds is particularly

widespread in China (Ren et al., 2019, Duan et al., 2020; Gao et al., 2019). The change from temporarily water-logged coastal wetlands to continuously flooded ponds can strongly affect sediment physicochemical properties and the subsequent CH_4 biogeochemical processes, but the relevant scientific data are rare.

We compared the sediment physicochemical properties, CH_4 production potentials and metagenomics of the methanogenic archaea communities between a coastal marsh and an area that had been converted to aquaculture ponds in southeastern China. Network analysis is a tool to examine changes in property and connectivity within a biological community (Barberán et al., 2012; Banerjee et al., 2021; Liu et al., 2021a; Zhou et al., 2020), including soil microbial communities (Chen et al., 2019; Qiu et al., 2021). Here, we applied network analysis to the metagenomics data to characterize differences in the sediment methanogenic archaea community between marsh land and aquaculture ponds. This study helped us understand the effects of LULCC on sediment methanogenic archaea community, its CH_4 production potential and related climate impact.

2. Materials and methods

2.1. Study area

The Shanyutan Wetland (26°00′36″–26°03′42″ N, 119°34′12″–119°40′40″ E), located at the mouth of the Min River Estuary in southeastern China (Figure 1), has a subtropical monsoonal climate with an annual average temperature of 19.6 °C and precipitation of 135 cm (Yang et al., 2017a). The semidiurnal tidal range is 0.1–1.5 m (Tong et al., 2018); the average salinity is 4.2±2.5 parts per thousand (ppt) (Yang et al., 2019a). Aquaculture shrimp ponds, common in the area, were reclaimed from nearby marsh land in 2011 by removing the vegetation (predominantly *Cyperus malaccensis*) and re-profiling the bunds into steep slopes (Powell et al., 2020; Yang et al., 2020a).

These ponds cover approximately 30% of the total area of the Shanyutan Wetland. Details about the aquaculture pond system and the management practices can be found in Yang et al. (2017b; 2020b; 2021). For this study, a brackish *C. malaccensis* marsh stand and three aquaculture ponds were selected (Figure 1) for sampling between April 2019 and January 2020.

2.2. Sediment porewater collection and analysis

Within the marsh stand, we established three quadrats (1 m × 1 m) with 2 m spacing. Sediment porewater was sampled by *in situ* dialysis (Ding et al., 2003; Strack and Waddington, 2008; Tong et al., 2018). Three screened (Biotrans™ 0.2 μm nylon membrane, Tong et al., 2018) PVC tubes (5 cm inner diameter) extending 15 cm into the sediment were permanently installed in each quadrat, leaving a 5-cm protrusion above the sediment surface. The top of each tube was sealed when submerged and was only opened during neap tides for extracting the porewater (Yang et al., 2019b).

Sediment cores (15 cm length) were collected from three sites in each aquaculture pond using a steel sediment sampler (internal diameter 5 cm). Porewater was extracted from the pond sediment by centrifugation (4,000 rpm, 10 min Hereaus Omnifuge 2000 RS) (Matos et al., 2016).

Field sampling were carried out monthly from April 2019 to January 2020. All samples were stored in an ice box and transported to the laboratory within 6 h. Approximately 50 mL of each porewater sample was filtered through a 0.45 μm filter (Biotrans™ nylon membranes) (De Vittor et al., 2012), and the filtrate was analyzed for the concentrations of dissolved organic carbon (DOC), Cl^{-1} and SO_4^{2-}. Porewater DOC concentrations were determined by a Schimadzu TOC-$V_{CPH/CPN}$ analyzer (Kyoto, Japan). Porewater Cl^{-1} and SO_4^{2-} concentrations were measured by a Dionex 2100 ion chromatograph.

2.3. Sediment sampling and physicochemical properties

During each sampling campaign, triplicate surface sediment samples (top 15 cm) were collected from the aforementioned locations with a steel sediment sampler (internal diameter 5 cm) and transferred into ziplock bags. All sediment samples were stored in an ice box and transported to the laboratory within 6 h. In the laboratory, the triplicate sediment samples from each site were used respectively for incubation experiment, measurement of sediment physicochemical properties, and analysis of sediment microorganisms. Sediment temperature (T_S) and electrical conductivity (EC) were measured *in situ* using a handheld temperature meter (IQ150, IQ Scientific Instruments, USA) and a 2265FS EC meter (Spectrum Technologies, USA), respectively.

In the laboratory, the sediment samples were diluted with deionized water before measuring sediment pH (Orion 868 pH meter, USA; sediment-to-water ratio 1:2.5 w/v) and salinity (Eutech Instruments-Salt6 salinity meter, USA; sediment-to-water ratio 1:5 w/v) (Liu et al., 2021b); readings were subsequently corrected for the dilution effects. A subsample of the sediment was freeze-dried, homogenized and then ground to a fine powder for measuring total carbon (TC) and total nitrogen (TN) by an elemental analyzer (Elementar Vario MAX CN, Germany). Another subsample was weighed, oven-dried for 48 hours, then re-weighed to obtain the moisture content.

2.4. Illumina sequencing and bioinformatics analysis

Triplicate sediment samples collected from the marsh and each of the aquaculture ponds in May, August, October and January were used for metagenomics, giving a total of 12 samples for the marsh and 36 samples for the aquaculture ponds. The 16S rRNA gene for methanogenic archaea was combined with adaptor sequences and barcode sequences in PCR amplification using the primer pair 1106F

(TTWAGTCAGGCAACGAGC) and 1378R (TGTGCAAGGAGCAGGGAC) (Li et al., 2021). For each of the 48 sediment DNA samples, the PCR was performed in triplicate and the PCR products were pooled subsequently. Afterward, the amplicons were extracted in 2% agarose gels and purified using the AxyPrep DNA Gel Extraction Kit (Axygen, USA) according to the manufacturer's instructions, and quantified using QuantiFluor™-ST (Promega, U.S.). Purified amplicons were pooled equimolar and paired-end sequenced (2 × 250) on Illumina MiSeq PE300 platform by the standard protocols. The processing of raw fastq files followed previous study (Ye et al., 2021). Operational Taxonomic Units (OTUs) were classified as clusters with 97% similarity cutoff using the Ribosomal Database Project (RDP) classifier within the SILVA database (Quast et al., 2013). To ensure OTU data compatibility between samples, sequences were rarefied to the lowest number of reads. The alpha diversity indices, including Chao1 index, OTU richness, phylogenetic diversity index and Shannon index were calculated using QIIME software (Caporaso et al., 2010; Chen et al., 2015). OTUs affiliated to methanogenic archaea were selected for network analysis (section 2.6).

2.5. Sediment CH_4 production potential

Anaerobic incubation experiments were conducted to measure sediment CH_4 production potential (Bodmer et al., 2020; Liu et al., 2011; Inglett et al., 2012; Minick et al., 2021). Approximately 30 g of each sediment sample was put into a 200 mL glass incubation bottle and *in situ* water was added in 1:1 v/v to make a slurry with 160 mL headspace. Before the start of incubation, the bottles were flushed with pure nitrogen gas (N_2) for 5–8 min to create an anoxic condition (Wassmann et al., 1998; Vizza et al., 2017; Zhou et al., 2022). The bottles were then incubated at in *situ* temperature (14–30 ^{o}C) for 15 days. We collected 5 mL gas samples from the headspace with a syringe every two days over the incubation period (total 8 times). For each gas sampling, 5 mL of pure N_2

gas was added back into the incubation bottles to maintain the pressure. The extracted gas samples were analyzed for CH_4 on a gas chromatograph equipped with a flame ionization detector (GC-2010, Shimadzu, Japan). Sediment CH_4 production potential was calculated from the increase in headspace CH_4 concentration in each incubation bottle (corrected for dilution effect from the added N_2) over the 15-day period with the following Eq. (1) (Wassmann et al., 1998):

$$PP = \frac{dc}{dt} \bullet \frac{M_M \times V_H \times P_A}{R \times W_S} \bullet \frac{T_{ST}}{T_{ST}+T} \quad \text{(Eq.1)}$$

where PP is the sediment CH_4 production potential [μg CH_4 g^{-1} (dry weight) day^{-1}]; dc/dt is the rate of change in headspace CH_4 in the incubation bottle over time (mmol mol^{-1} d^{-1}); M_M is the molar mass (g mol^{-1}) of CH_4 (g); V_H is the volume of serum bottles headspace (L); P_A is the atmospheric pressure (kPa); R is the gas constant (m^3 Pa $°K^{-1}$ mol^{-1}); W_S is the dry weight of soil sample (g); T_{ST} and T are the standard temperature (°K) and the incubation temperature (°K), respectively. The sediment dry weight was estimated from the sample wet weight and its moisture content (see section 2.3).

2.6. Data analysis

Nonmetric multidimensional scaling (NMDS) analysis was done in RStudio using the Bray-Curtis similarity matrix calculated based on OTUs. Analysis of similarities (ANOSIM) was used to assess the community composition differences between the sample groups. The ANOSIM R statistic value of "0" indicates completely random grouping, and "1" indicates a complete separation between sample groups. In addition, permutation multivariate analysis of variance (PerMANOVA) was performed to test for significant differences between the sample groups using the R "vegan" package (Chen et al., 2019), with Bray-Curtis distance and 999 permutations.

The associations between predictor index (sediment properties and microbial diversity)

and CH_4 production potential were evaluated by Random Forest Analysis (RFA), using the "RandomForest" package in R. RFA evaluated the importance of each predictor by determining how much the mean square error (MSE) increased. For this study, the significance of both the model and each predictor was assessed with the "rfPermute" packages. The differences in sediment CH_4 production potential and environmental variables between the marsh and the aquaculture ponds were tested by repeated measures ANOVA analysis followed by *Tukey*'s posthoc test. Statistical analyses were conducted in SPSS 17.0 (SPSS Inc., USA). All results were presented as the mean ± standard error.

To reduce the complexity of the data sets for network analysis, OTUs present in more than eight samples with relative abundance greater than 0.1% were retained for the construction of networks. Subsequently, all possible pairwise Spearman's rank correlations (r) between those OTUs were calculated within the "Hsmic" R package. Species co-occurrences were included in the networks only where correlations between species were robust ($r^2 > 0.49$) and statistically significant ($p < 0.01$, adjusted by FDR). Network visualization and modular analysis were done in Gephi version 0.9.1 platform, with nodes representing OTUs, edges indicating correlations between two OTUs, and degrees indicating the sum of edges that connect with other nodes. Sub-networks for each sample were extracted by preserving the topological parameters of individual sediment samples, using the "induced_subgraph" function in the "igraph" package in R (Ma et al., 2016). Thereafter, we calculated the connectivity for the subnetworks within each habitat. Statistical differences in measured node-level attributes between the two habitats were tested by nonparametric Mann–Whitney U test.

Results

3.1. Physicochemical properties of sediment

The marsh and the aquaculture ponds differed substantially in sediment properties (Figure 2). The mean sediment T_S, salinity and EC in the marsh was 24.70 ± 0.85 ºC, 6.69 ± 0.63‰ and 4.71 ± 0.51 μS cm^{-1}, respectively, all significantly higher than the corresponding values in the pond sediment (20.42 ± 0.62 ºC, 2.51 ± 0.16‰ and 2.36 ± 0.15 μS cm^{-1}; ANOVA, $p < 0.05$ or <0.01; Figure 2a, c, d). The sediment TC and TN contents in the marsh were 20.18 ± 1.78 g kg^{-1} and 1.34 ± 0.09 g kg^{-1}, respectively, which were significantly higher than those in the pond sediment (TC: 16.51 ± 1.33 g kg^{-1} and TN: 0.70 ± 0.07 g kg^{-1}; ANOVA, $p < 0.05$; Figure 2e, f). Furthermore, the porewater DOC concentration and Cl^- concentration were also significantly higher in the marsh than in the ponds (DOC: 18.27 ± 0.80 *vs* 6.83± 0.86 mg L^{-1}; Cl^-: 5436 ± 676 *vs* 2690 ± 345 mg L^{-1}; ANOVA, $p < 0.01$; Figure 2g, h). There were no significant differences in sediment pH (6.72 ± 0.12 *vs* 6.75± 0.04; Figure 2b) or porewater SO_4^{2-} concentration (935.24 ± 98.61 mg L^{-1} *vs* 780.38 ± 78.51 mg L^{-1}; Figure 2i) between the two habitats (ANOVA, $p > 0.05$). The seasonal values of physicochemical parameters of the sediments are shown in Figure S1.

3.2. Diversity and compositions of sediment methanogenic archaea communities

The diversity of sediment methanogenic archaea communities in the marsh and the aquaculture ponds were evaluated in terms of OTU richness, Chao1, phylogenetic diversity and Shannon indices (Figure 3). The alpha diversity was significantly lower in the aquaculture ponds than in the marsh by all measures ($p < 0.05$, < 0.01 or < 0.001; Figure 3).

The top 10 genera of methanogenic archaea in the samples are shown in Figure 4a. In the marsh sediment, the methanogenic archaea community was dominated by *Methanobacterium* (58.6%), followed by *Methanosphaera* (13.1%), *Methanocella*

(7.0%), *Methanosarcina* (6.5%) and *Methanolobus* (3.1%). In the pond sediment, the methanogenic archaea community was dominated by *Methanobacterium* (40.6%), followed by *Methanosphaera* (17.2%), *Methanosarcina* (13.8%) and *Methanocella* (10.5%). NMDS analysis revealed a significant ($p < 0.001$) difference in sediment methanogenic archaea community compositions between the two habitats (Figure 4b).

3.3. Co-occurrence networks of sediment methanogenic archaea

Networks of the methanogenic archaea were constructed at the OTU level across all sediment samples. The network consisted of 215 nodes linked by 928 edges (Figure 5). Furthermore, we compared the microbial network complexity between the two habitats based on their node-level topological features: Significantly lower node number (Figure 6a) and degree (Figure 6b) values were found in the aquaculture ponds than in the marsh ($p < 0.001$), suggesting a lower complexity of the sediment microbial community network in the aquaculture ponds. Concurrently, network complexity both in terms of node number and degree was strongly correlated ($p < 0.05$) with CH_4 production potential (Figure 6c and 6d).

3.4. Sediment CH_4 production potential

The monthly sediment CH_4 production potential ranged from 3.34 ± 0.66 ng g^{-1} d^{-1} to 134.16 ± 28.35 ng g^{-1} d^{-1} in the marsh and from 3.38 ± 0.86 ng g^{-1} d^{-1} to 52.74 ± 11.40 ng g^{-1} d^{-1} in the aquaculture ponds (Figure 7). The mean value for the marsh (45.21 ± 12.73 ng g^{-1} d^{-1}) was significantly higher than that for the aquaculture ponds (20.14 ± 5.59 ng g^{-1} d^{-1}) ($F_{df=1}=7.251$, $p=0.009$). When comparing across seasons, the CH_4 production potential in both habitats were substantially higher in summer and autumn than in spring and winter (Figure S2).

Pearson correlation analysis showed that the sediment CH_4 production potential was

not correlated with pH in either habitat (Table 1), but it was positively correlated with T_S, TC and DOC concentration (also TN in marsh sediment), and negatively with salinity, EC, Cl^- concentration and SO_4^{2-} concentration (Table 1). Furthermore, positive correlations were found between sediment CH_4 production potential and all four measures of alpha diversity of sediment methanogenic archaea across the two habitats ($p < 0.01$; Figure S3).

Based on the result of RFA, sediment TC, porewater SO_4^{2-} concentration, T_S and methanogenic archaea richness were the variables that best explained the variations in sediment CH_4 production potential, of which TC accounted for the highest percentage (Figure 8).

4. Discussion

4.1. Temporal patterns of CH_4 production potential in marsh sediment

Our results showed that CH_4 production potential in marsh sediment was significantly higher in the summer and autumn (Figure S2), similar to the observations in other wetlands (e.g., Bergman et al., 2000; Tong et al., 2012; Vizza et al., 2017). Other researchers have attributed this to the seasonal variations in temperature that drive the production of substrate precursors and microbial activity (Zogg et al., 1997; Bergman et al., 2000; Gudasz et al., 2010; Inglett et al., 2012). Similarly, we also found that T_S, TC and porewater DOC concentration were all higher in summer and autumn (Figure S1), and they were all significantly and positively correlated with sediment CH_4 production potential (Table 1).

Salinity was another important driver of the seasonal variability of sediment CH_4 production potential. Significant effects of saltwater have been observed in coastal marshes in several studies showing decreased sediment CH_4 production as salinity

increased (e.g., Baldwin et al., 2006; Minick et al., 2019; Vizza et al., 2017). Salt water intrusion increases the availability of the more energetically favorable terminal electron acceptor such as SO_4^{2-} in the sediment, which allows sulfate-reducing bacteria to outcompete methanogens (e.g., Bridgham et al., 2013; Chambers et al., 2013; Dang et al., 2019; Neubauer et al., 2013; Poffenbarger et al., 2011). This may explain the negative correlations of sediment CH_4 production potential with salinity, SO_4^{2-} concentration, EC and Cl^- concentration (Table 1), and why sediment CH_4 production potentials in the two habitats were significantly higher in the summer months when saltwater influence was weakened (Figure S1c, d, h) by high precipitation and runoff (Figure S4).

Across our sampling period, the sediment CH_4 production potentials averaged 45.2 ng g^{-1} d^{-1} (marsh) and 20.1 ng g^{-1} d^{-1} (aquaculture ponds). These values were much lower than that of eutrophic sediments (Berberich et al., 2020), but comparable to that of oligo- to meso-trophic sediments (Fuchs et al., 2016), and they are within the range reported for similar habitats (Tong et al., 2015).

4.2. Changes in sediment methanogenic archaea community structures

Previous studies have shown that the composition and functionality of soil and sediment microbiota are sensitive to anthropogenic disturbances and environmental changes (e.g., Bragazza et al., 2013; Peltoniemi et al., 2016; Hellman et al., 2019; Cui et al., 2021). In the present study, we assessed the effect of LULCC by comparing the sediment methanogenic archaea community composition and CH_4 production potential between a brackish marsh and the nearby area that had been converted to aquaculture ponds. An interesting finding was that the sediment methanogenic archaea community was significantly less diverse in the ponds than in the marsh (Figure 3), indicating that the land conversion negatively impacted some of the sediment methanogenic archaea.

309 Conversion of the marsh to aquaculture ponds also affected the dominant
310 methanogenic archaea taxa at the genus level. *Methanobacterium* was by far the most
311 abundant (ca. 59%) in the marsh sediment, followed by *Methanosphaera* (Figure 4a). In
312 pond sediment, *Methanobacterium* was also prevalent but less dominant (ca. 41%);
313 *Methanosphaera* and *Methanocella* were also quite abundant. Most notably,
314 *Methanosarcina* formed a higher percentage of the methanogenic archaea community in
315 the ponds than in the marsh (Figure 4a). Among these genera, *Methanobacterium*,
316 *Methanosphaera* and *Methanocella* are hydrogenotrophic methanogens that can utilize
317 both formate and H_2/CO_2 to produce methane (Jeanlouis et al., 2000; Wang et al., 2016),
318 whereas *Methanosarcina* is facultative methanogen that can utilize H_2/CO_2, methyl
319 compounds, and/or acetate to produce methane (Ferry, 2010). Our results therefore
320 suggest that methanogenesis changed from a predominantly hydrogenotrophic pathway
321 in the marsh sediment to a mix of different pathways in the pond sediment.
322 Network analysis has been successfully used to study soil microbial community
323 structures and assess their changes due to disturbances (Barberán et al., 2012; Chen et al.,
324 2019; Qiu et al., 2021). Here, we applied this technique to explore the effects of land
325 conversion on the co-occurrence patterns of sediment methanogenic archaea
326 communities. Our results showed that the marsh sediment had a significantly higher
327 microbial network complexity (Figure 6a and 6b) than the aquaculture pond sediment
328 (p<0.001), suggesting that the methanogenic archaea were more interconnected with one
329 another in the former than in the latter. Taken together, our results indicate that the
330 conversion of marsh land to aquaculture ponds led to a simpler methanogenic archaea
331 community structure, and presumably a lower degree of microbial cooperation in the
332 sediment (Ju et al., 2014) that may have led to lower CH_4 production.
333 *4.3. Changes in sediment physicochemical properties*

RFA results show that the sediment CH_4 production potential was strongly driven by sediment carbon content (TC), which explained nearly 15% of the variations (Figure 8). This was followed by sulfate concentration (SO_4^{2-}), temperature (T_S) and methanogenic archaea species richness. TC is indicative of substrate availability that fuels methanogenesis (Updegraff et al., 1995; Liu et al., 2011; Song et al., 2021), whereas T_S affects the overall microbial activity (Bergman et al., 2000; Gudasz et al., 2010; Inglett et al., 2012), and a higher species richness would allow the methanogenic archaea community to exploit a wider range of ecological niches (Godin et al., 2012). Hence, it is no surprise that these three parameters were positively correlated with CH_4 production potential (Table 1). Sulfate reducers tend to outcompete methanogenic archaea for electron donors (Vizza et al., 2017; dos Santos Fonseca et al., 2019); therefore, higher SO_4^{2-} concentration would lead to a lower CH_4 production potential (Table 1). The differences in these key sediment properties between the marsh and the aquaculture ponds may explain the different CH_4 production potentials observed in the incubation experiments: Pond sediment had lower TC, higher SO_4^{2-} concentration (summer), lower T_S (Figure S1) and lower species richness (Figure 3) than marsh sediment. Consequently, the CH_4 production potential in the pond sediment was only 44% of that in the marsh sediment (Figure 7).

4.4. Effects of land conversion on sediment CH_4 production

The continuous river flow and periodic tidal flushing within the marsh should increase the dissolved oxygen level that suppresses methanogenic archaea activity, promotes CH_4 oxidation and minimizes CH_4 accumulation within the water column. In contrast, the stagnant nature of the pond water means should favor sediment CH_4 production and accumulation, leading to a high emission (Tan et al., 2020; Yang et al.,

358 2017a). Therefore, the increasing conversion of coastal wetlands to aquaculture ponds
359 raises the concern of changing (increasing) the production and subsequent release of
360 greenhouse gases (Yuan et al., 2019a). Interestingly, based on incubation experiments,
361 we found that the mean CH_4 production potential in pond sediment was significantly
362 lower than that in marsh sediment.

363 Contrary to the common expectation that use of aquaculture feeds would elevate the
364 sediment carbon content in the ponds, TC was actually higher in the marsh particularly
365 in the summer and autumn (Figure S1), when most of the CH_4 production occurred
366 (Figure S2). In addition to carbon supply from marsh vegetation and other autochthonous
367 sources, the marsh also receives nutrients and organics from the Min River, which
368 together can stimulate sediment CH_4 production. The higher water level within the
369 aquaculture ponds may have also buffered the sediment against temperature rise in the
370 summer (Figure S1), leading to a lower CH_4 production potential. Some of the native
371 microbes in marsh sediment may not be able to adapt to the very different
372 physicochemical environments in the ponds, and the common practice of draining, drying
373 and liming the ponds between farming periods would have further disrupted the sediment
374 microbial community (Tong et al., 2021). This may explain the overall lower
375 methanogenic archaea diversity (Figure 3) and less complex community structure in the
376 pond sediment (Figure 5), and perhaps leads to the lower CH_4 production potential as a
377 result (Figure 6c and 6d).

378 *4.5. Limitations and future research*

379 Our study examined the effects of conversion of coastal wetland to aquaculture
380 ponds on sediment CH_4 production potential over an annual cycle. Several aspects could
381 be investigated further in future studies. Firstly, coastal LULCC often involves

conversion for multiple land-use types rather than a single land-use type (Tan et al., 2020). Therefore, future research may require detailed comparison of multiple habitat types within the same locale. Furthermore, we conducted our study in shrimp ponds, whereas other aquaculture systems and species may induce different microbial communities and different sediment and water biogeochemistry. Comparative studies of different aquaculture practices in different regions would produce a more comprehensive understanding of the overall impacts of the aquaculture industry on climate (MacLeod et al., 2020). While in the present study we only analyzed the sediment methanogenic archaea community compositions, incorporation of isotopic measurements of the gases would shed light on the methanogenic pathways involved (Qin et al., 2020; Yang et al., 2020; Yuan et al., 2019b). Lastly, the apparent contradiction between the observed sediment CH_4 production potentials and the water-to-air CH_4 emission reported earlier need to be resolved by investigating the fate of CH_4 in the water column and the pathways to transport sediment CH_4 to air.

5. Conclusions

Conversion of coastal wetland to aquaculture ponds is widespread in coastal China and is expected to increase in order to meet the rising food demand. This study was the first to show the change in sediment CH_4 production potential and sediment microbial community structure following the conversion of a brackish marsh to aquaculture ponds in subtropical China. Contrary to the common expectation, our results showed that the conversion decreased the sediment methanogenic archaea diversity, disrupted the microbial community structure, and decreased the capacity for CH_4 production in the sediment. These findings point to the need for a more careful consideration when assessing the effects of land use and land cover change on greenhouse gas dynamics.

Declaration of competing interest

The authors declare that they have no known competing financial interests or personal relationships that could have appeared to influence the work reported in this paper.

Acknowledgements

This research was funded jointly by the National Natural Science Foundation of China (NSFC) (grant numbers: 41801070, 41671088), and the National Natural Science Foundation of Fujian Province of China (grant numbers: 2020J01136, 2018J01737).

References

Andreetta, A., Huertas, A.D., Lotti, M., Cerise, S., 2016. Land use changes affecting soil organic carbon storage along a mangrove swamp rice chronosequence in the Cacheu and Oio regions (northern Guinea-Bissau). Agr. Ecosyst. Environ. 216, 314–321. https://doi.org/10.1016/j.agee.2015.10.017

Baldwin, D.S., Rees, G.N., Mitchell, A.M., Watson, G., Williams, J., 2006. The short-term effects of salinization on anaerobic nutrient cycling and microbial community structure in sediment from a freshwater wetland. Wetlands 26, 455–464.

Banerjee, S., Zhao, C., Kirkby, C.A., Coggins, S., Zhao, S., Bissett, A., van der Heijden, Marcel G.A., Kirkegaard., J., Richardson, A.A.E., Microbial interkingdom associations across soil depths reveal network connectivity and keystone taxa linked to soil fine-fraction carbon content. Agr. Ecosyst. Environ. 320, 10755. https://doi.org/10.1016/j.agee.2021.107559

Barberán, A., Bates, S.T., Casamauor, E.O., Fierer, N., 2012. Using network analysis to explore co-occurrence patterns in soil microbial communities. ISME J. 6, 343–351. https://doi.org/10.1038/ismej.2011.119

Barbier, E.B., Hacker, S.D., Kennedy, C., Koch, E.W., Stier, A.C., Silliman, B.R., 2011. The value of estuarine and coastal ecosystem services. Ecol. Monogr. 81, 169–193. https://doi.org/10.1890/10-1510.1

Berberich, M.E., Beaulieu, J.J., Hamilton, T.L., Waldo, S., Buffam, I., 2020. Spatial variability of sediment methane production and methanogen communities within a eutrophic reservoir:

Importance of organic matter source and quantity. Limnol. Oceanogr. 65, 1336–1358. https://doi.org/10.1002/lno.11392

Bergman, I., Klarqvist, M., Nilsson, M., 2000. Seasonal variation in rates of methane production from peat of various botanical origins: effects of temperature and substrate quality. FEMS Microbiol. Ecol. 33, 181–189. https://doi.org/10.1016/s0168-6496(00)00060-x

Bodmer, P., Wilkinson, J., Lorke, A., 2020. Sediment properties drive spatial variability of potential methane production and oxidation in small streams. J. Geophys. Res.-Biogeo. 125(1), e2019JG005213. https://doi.org/10.1029/2019JG005213

Bragazza, L., Parisod, J., Buttler, A., Bardgett, R.D., 2013. Biogeochemical plant–soil microbe feedback in response to climate warming in peatlands. Nat. Clim. Change 3, 273–277. https://doi.org/10.1038/NCLIMATE1781

Bridgham, S.D., Cadillo-Quiroz, H., Keller, J.K., and Zhuang, Q., 2013. Methane emissions from wetlands: biogeochemical, microbial, and modeling perspectives from local to global scales, Glob. Change Biol., 19, 1325–1346. https://doi.org/10.1111/gcb.12131

Caporaso, J.G., Kuczynski, J., Stombaugh, J., Bittinger, K., Bushman, F.D.,costello, E.K., Fierer, N., Peña, A.G., Goodrich, J.K., Gordon, J.I., Huttley, G.A., Kelley, S.T., Knights, D., Koenig, J.E., Ley, R.E., Lozupone, C.A., Mcdonald, D., Muegge, B.D., Pirrung, M., Reeder, J., Sevinsky, J.R., Turnbaugh, P.J., Walters, W.A., Widmann, J., Yatsunenko, T.Y., Zaneveld, J., Knight, R., 2010. QIIME allows analysis of high-throughput community sequencing data. Nat Methods 7, 335–336. https://doi.org/10.1038/nmeth.f.303

Chambers, L.G., Osborne, T.Z., Reddy, K.R., 2013. Effect of salinity-altering pulsing events on soil organic carbon loss along an intertidal wetland gradient: A laboratory experiment. Biogeochemistry 115(1–3), 363–383. https://doi.org/10.1007/s10533-013-9841-5

Chen, D., Wang, C., Li, Y., Liu, X.L., Wang, Y., Qin, J.Q., Wu, J.S., 2021. Effects of land-use conversion from Masson pine forests to tea plantations on net ecosystem carbon and greenhouse gas budgets. Agr. Ecosyst. Environ. 320, 107578. https://doi.org/10.1016/j.agee.2021.107578

Chen, J.H., Liu, X.Y., Li, L.Q., Zheng, J.W., Qu, J.J., Zheng, J.F., Zhang, X.H., Pan, G.X., 2015. Consistent increase in abundance and diversity but variable change in community composition of bacteria in topsoil of rice paddy under short term biochar treatment across three sites from South China. Appl. Soil Ecol. 91, 68–79. https://doi.org/10.1016/j.apsoil.2015.02.012

Chen, L.J., Jiang, Y.J., Liang, C., Luo, Y., Xu, Q.S., Han, C., Zhao, Q.G. Sun, B., 2019. Competitive interaction with keystone taxa induced negative priming under biochar amendments. Microbiome 7, 77. https://doi.org/10.1186/s40168-019-0693-7

Chmura, G.L., Anisfeld, S.C., Cahoon, D.R., Lynch, J.C., 2003. Global carbon sequestration in tidal, saline wetland soils. Glob. Biogeochem. Cycles 17, 1111. https://doi.org/10.1029/2002GB001917

Cui, J.L., Glatzel, S., Bruckman, V.J., Wang, B.Z., Lai, D.Y.F., 2021. Long-term effects of biochar application on greenhouse gas production and microbial community in temperate forest soils under increasing temperature. Sci. Total Environ. 767, 145021. https://doi.org/10.1016/j.scitotenv.2021.145021

De Vittor, C., Faganeli, J., Emili, A., Covelli, S., Predonzani, S., Acquavita, A., 2012. Benthic fluxes of oxygen, carbon and nutrients in the Marano and Grado Lagoon (northern Adriatic Sea, Italy). Estuarine, Estuar. Coast. Shelf S. 113, 57–70. https://doi.org/10.1016/j.ecss.2012.03.031

Dick, T.M., Osunkoya, O.O., 2000. Influence of tidal restriction floodgates on decomposition of mangrove litter. Aquat. Bot. 68, 273–280. https://doi.org/10.1016/S0304-3770(00)00119-4

Ding, W.X., Cai, Z.C., Tsuruta, H., Li, X.P., 2003. Key factors affecting spatial variation of methane emissions from freshwater marshes. Chemosphere 51, 167–173. https://doi.org/10.1016/S0045-6535(02)00804-4

dos Santos Fonseca, A.L., Marinho, C.C., de Assis Esteves, F., 2019. Acetate and sulphate as regulators of potential methane production in a tropical coastal lagoon. J. Soil. Sediment. 19, 2604–2612. https://doi.org/10.1007/s11368-019-02249-y

Dang, C., Morrissey, E.M., Neubauer, S.C., and Franklin, R.B., 2019. Novel microbial community composition and carbon biogeochemistry emerge over time following saltwater intrusion in wetlands. Glob. Change Biol. 25, 549–561. https://doi.org/10.1111/gcb.14486

Doroski, A.A., Helton, A.M., Vadas, T.M., 2019. Greenhouse gas fluxes from coastal wetlands at the intersection of urban pollution and saltwater intrusion: A soil core experiment. Soil Biol. Biochem. 41, 2501–2507. https://doi.org/10.1016/j.soilbio.2009.09.008

Duan, Y.Q., Li, X., Zhang, L.P., Chen, D., Liu, S.A., Ji, H.Y., 2020. Mapping national-scale aquaculture ponds based on the Google Earth Engine in the Chinese coastal zone. Aquaculture 520, 734666. https://doi.org/10.1016/j.aquaculture.2019.734666

494 Ferry, J.G., 2010. How to make a living by exhaling methane. Annual Review of Microbiology 64,
495 453–73. https://doi.org/10.1146/annurev.micro.112408.134051
496 Fuchs, A., Lyautey, E., Montuelle, B., Casper, P., 2016. Effects of increasing temperatures on methane
497 concentrations and methanogenesis during experimental incubation of sediments from
498 oligotrophic and mesotrophic lakes. J. Geophys. Res.-Biogeo. 121, 1394–1406.
499 https://doi.org/10.1002/2016JG003328
500 Gao, D.Z., Liu, M., Hou, L.J., Lai D.Y.F., Wang, W.Q., Li, X.F., Zeng, A.Y., Zheng, Y.L., Han, P.,
501 Yang, Y., Yin, G.Y., 2019. Effects of shrimp-aquaculture reclamation on sediment nitrate
502 dissimilatory reduction processes in a coastal wetland of southeastern China. Environ. Pollut.
503 255, 113219. https://doi.org/10.1016/j.envpol.2019.113219
504 Godin, A., McLaughlin, J. W., Webster, K. L., Packalen, M., Basiliko, N., 2012. Methane and
505 methanogen community dynamics across a boreal peatland nutrient gradient. Soil Biol. Biochem.
506 48, 96–105. https://doi.org/10.1016/j.soilbio.2012.01.018
507 Gruca-Rokosz, R., Szal, D., Bartoszek, L., Pękala, A., 2020. Isotopic evidence for vertical
508 diversification of methane production pathways in freshwater sediments of Nielisz reservoir
509 (Poland). Catena 195, 104803. https://doi.org/10.1016/j.catena.2020.104803
510 Gudasz, C., Bastviken, D., Steger, K., Premke, K., Sobek, S., Tranvik, L.J., 2010. Temperature
511 controlled organic carbon mineralization rates in lakes. Nature 466, 478–481.
512 https://doi.org/10.1038/nature09186
513 Han, G.X., Xing, Q.H., Yu, J.B., Luo, Y.Q., Li, D.J., Yang, L.Q., Wang, G.M., Mao, P.L., Xie, B.H.,
514 Mikle, N., 2014. Agricultural reclamation effects on ecosystem CO2 exchange of a coastal
515 wetland in the Yellow River Delta. Agr. Ecosyst. Environ. 196, 187-198.
516 https://doi.org/10.1016/j.agee.2013.09.012
517 Hao, J., Xu, G.Y., Luo, , Zhang, Z., Yang, H. L., Li, H. Y., 2020. Quantifying the relative contribution
518 of natural and human factors to vegetation coverage variation in coastal wetlands in China.
519 Catena 188, 104429. https://doi.org/10.1016/j.catena.2019.104429
520 Hellman, M., Bonilla-Rosso, G., Widerlund, A., Juhanson, J., Hallin, S., 2019. External carbon
521 addition for enhancing denitrification modifies bacterial community composition and affects
522 CH_4 and N_2O production in sub-arctic mining pond sediments. Water Res. 158, 22–33.
523 https://doi.org/10.1016/j.watres.2019.04.007

Huang, Y., Sun, W.J., Zhang, W., Yu, Y.Q., Su, Y.H., Song, C.C., 2010. Marshland conversion to cropland in northeast China from 1950 to 2000 reduced the greenhouse effect. Glob. Change Biol. 16, 680–695. https://doi.org/10.1111/j.1365-2486.2009.01976.x

Inglett, K.S., Inglett, P.W., Reddy, K.R., Osborne, T.Z., 2012. Temperature sensitivity of greenhouse gas production in wetland soils of different vegetation. Biogeochemistry 108, 77–90. https://doi.org/10.1007/s10533-011-9573-3

IPCC, 2013. Climate Change 2013: The Physical Science Basis. In: Stocker, T.F. (Ed.), Contribution of Working Group I to the Fifth Assessment Report of the Intergovernmental Panel on Climate Change. Cambridge Univ. Press. https://doi.org/10.1017/CBO9781107415324

Jeanlouis, G., Bharat, K.C.P., Bernard, O., 2000. Taxonomic, phylogenetic, and ecological diversity of methanogenic archraea. Anaerobe 6, 205–226. https://doi.org/10.1006/anae.2000.0345

Ju, F., Xia, Y., Gou, F., Wang, Z.P., Zhang, T., 2014. Taxonomic relatedness shapes bacterial assembly in activated sludge of globally distributed wastewater treatment plants. Environ Microbiol. 16, 2421–2432. https://doi.org/10.1111/1462-2920.12355

Li, B.B., Roley, S.S., Duncan, D.S., Guo, J.R., Quensen, J.F., Yu, H.Q., Tiedje, J.M., 2021. Long-term excess nitrogen fertilizer increases sensitivity of soil microbial community to seasonal change revealed by ecological network and metagenome analyses. Soil Biol. Biochem. 160, 108349. https://doi.org/10.1016/j.soilbio.2021.108349

Liu, C., Li, H., Zhang, Y.Y., Si, D.D., Chen, Q.W., 2016. Evolution of microbial community along with increasing solid concentration during high solids anaerobic digestion of sewage sludge. Bioresour. Technol. 216, 87–94. http://dx.doi.org/10.1016/j.biortech.2016.05.048

Lai, D.Y.F., 2009. Methane dynamics in northern peatlands: A review. Pedosphere 19, 409–421. https://doi.org/10.1016/S1002-0160(09)00003-4

Liu, D.Y., Ding, W.X., Jia, Z.J., Cai, Z.C., 2011. Relation between methanogenic archaea and methane production potential in selected natural wetland ecosystems across China. Biogeosciences 8, 329–338. https://doi.org/10.5194/bg-8-329-2011

Liu, J.G., Hartmann, S.C., Keppler, F., Lai, D.Y.F., 2019. Simultaneous abiotic production of greenhouse gases (CO_2, CH_4, and N_2O) in subtropical soils. J. Geophys. Res.-Biogeo. 124, 1977–1987. https://doi.org/10.1029/2019JG005154

Liu, J.L., Li, S.Q., Yue, S.C., Tian, J.Q., Chen, H., Jiang, H.B., Siddique, K.H.M., Zhan, A., Fang,

554 Q.X., Yu, Q., 2021. Soil microbial community and network changes after long-term use of plastic
555 mulch and nitrogen fertilization on semiarid farmland. Geoderma 396, 115086.
556 https://doi.org/10.1016/j.geoderma.2021.115086
557 Liu, Q., Mo, X., 2016. Interactions between surface water and groundwater: key processes in
558 ecological restoration of degraded coastal wetlands caused by reclamation. Wetlands 36 (Suppl.
559 1), S95–S102. https://doi.org/10.1007/s13157-014-0582-6
560 Liu, W., Shi, C., Ma, Y. Y., Li, H. J., Ma, X. Q., 2021a. Land use and land cover change-induced
561 changes of sediment connectivity and their effects on sediment yield in a catchment on the Loess
562 Plateau in China. Catena, 207, 105688. https://doi.org/10.1016/j.catena.2021.105688
563 Liu, Y., Yang, J.S., Ning, K., Wang, A.D., Wang, Q.X., Wang, X.H., Wang, S.W., Lv, Z.B., Zhao, Y.J.,
564 Yu, J.B., 2021b. Temperature sensitivity of anaerobic CO_2 production in soils of *Phragmites*
565 *australis* marshes with distinct hydrological characteristics in the Yellow River estuary. Ecol.
566 Indic. 124, 107409. https://doi.org/10.1016/j.ecolind.2021.107409
567 Lofton, D.D., Whalen, S.C., Hershey, A.E., 2015. Vertical sediment distribution of methanogenic
568 pathways in two shallow Arctic Alaskan lakes. Polar Biol. 38, 815–827.
569 https://doi.org/10.1007/s00300-014-1641-4
570 Ma, B., Wang, H.Z., Dsouza, M., Lou, J., He, Y., Dai, Z.M., Brookes, P.C., Xu, J.M., Gilbert, J.A.,
571 2016. Geographic patterns of co-occurrence network topological features for soil microbiota at
572 continental scale in eastern China. ISME J. 10, 1891–901.
573 https://doi.org/10.1038/ismej.2015.261
574 MacLeod, M.J., Hasan, M.R., Robb, D.H., Mamun-Ur-Rashid, M., 2020. Quantifying greenhouse gas
575 emissions from global aquaculture. Sci. Rep. 10, 1–8. https://doi.org/10.1038/s41598-020-
576 68231-8
577 Matos, C. R. L., Mendoza, U., Diaz, R., Moreira, M., Belem, A. L., Metzger, E., Albuquerque, A.L.S.,
578 Machado, W., 2016. Nutrient regeneration susceptibility under contrasting sedimentary
579 conditions from the Rio de Janeiro coast, Brazil. Mar. Pollut. Bull. 108, 297–302.
580 https://doi.org/10.1016/j.marpolbul.2016.04.046
581 Minick, K.J., Mitra, B., Li, X.F., Fischer, M., Aguilos, M., Prajapati, P., Noormets, A., King, J.S.,
582 2021. Wetland microtopography alters response of potential net CO_2 and CH_4 production to
583 temperature and moisture: Evidence from a laboratory experiment. Geoderma 402, 115367.

https://doi.org/10.1016/j.geoderma.2021.115367

Minick, K.J., Mitra, B., Noormets, A., King, J.S., 2019. Saltwater reduces potential CO_2 and CH_4 production in peat soils from a coastal freshwater forested wetland. Biogeosciences, 16, 4671–4686. https://doi.org/10.5194/bg-16-4671-2019

National Oceanic and Atmospheric Administration, 2020. Carbon cycle greenhouse gases: Trends in CH_4. Available in: https://www.esrl.noaa.gov/gmd/ccgg/trends_ch4/

Neubauer, S.C., Franklin, R.B., Berrier, D.J., 2013. Saltwater intrusion into tidal freshwater marshes alters the biogeochemical processing of organic carbon. Biogeosciences 10, 8171–8183. https://doi.org/10.5194/bg-10-8171-2013

Neubauer, S.C., Megonigal, J.P., 2015. Moving beyond global warming potentials to quantify the climatic role of ecosystems. Ecosystems 18, 1000–1013. https://doi.org/10.1007/s10021-015-9879-4

Peltoniemi, K., Laiho, R., Juottonen, H., Bodrossy, L., Kell, D.K., Minkkinen, K., Makiranta, P., Mehtatalo, L., Penttila, T., Siljanen, H.M.P., Tuittila, E.-S., Tuomivirta, T., Fritze, H., 2016. Responses of methanogenic and methanotrophic communities to warming in varying moisture regimes of two boreal fens. Soil Biol. Biochem. 97, 144–156. https://doi.org/10.1016/j.soilbio.2016.03.007

Poffenbarger, H.J., Needelman, B.A., Megonigal, J.P., 2011. Salinity influence on methane emissions from tidal marshes. Wetlands 31, 831–842. https://doi.org/10.1007/s13157-011-0197-0

Powell, E.B., Krause, J.R., Martin, R.M., Watson, E.B., 2020. Pond excavation reduces coastal wetland carbon dioxide assimilation. J. Geophys. Res.-Biogeo. 125, e2019JG005187. https://doi.org/10.1029/2019jg005187

Qin, X.B., Li, Y.E., Wan, Y.F., Fan, M.R., Liao, Y.L., Li, Y., Wang, B., Gao, Q.Z., Wu, H.B., Chen, X., 2020. Multiple stable isotopic signatures corroborate the predominance of acetoclastic methanogenesis during CH_4 formation in agricultural river networks. Agr. Ecosyst. Environ. 296, 106930. https://doi.org/10.1016/j.agee.2020.106930

Qiu, L.P., Zhang, Q., Zhu, H.S., Reich, P.B., Banerjee, S., van der Heijden, M. G. A., Sadowsky, M.J., Ishii, S., Jia, X.X., Shao, M.G., Liu, B.Y., Jiao, H., Li, H.Q., Wei, X.R., 2021. Erosion reduces soil microbial diversity, network complexity and multifunctionality. ISME J. 15, 2474–2489. https://doi.org/10.1038/s41396-021-00913-1

614 Quast, C., Pruesse, E., Yilmaz, P., Gerken, J., Schweer, T., Yarza, P., Peplies, J., Glockner, F.O., 2013.
615 The SILVA ribosomal RNA gene database project: improved data processing and web-based
616 tools. Nucleic Acids Research 41, D590–D596. https://doi.org/10.1093/nar/gks1219
617 Reay, D.S., Smith, P., Christensen, T.R., James, R.H., Clark, H., 2018. Methane and global
618 environmental change. Ann. Rev. Environ. Resour. 43, 165–192.
619 https://doi.org/10.1146/annurev-environ-102017-030154
620 Ren, C.Y., Wang, Z.M., Zhang, Y.Z., Zhang, B., Chen, L., Xia, Y.B., Xiao, X.M., Doughty, R.B., Liu,
621 M.Y., Jia, M., Mao, D.H., Song, K.S., 2019. Rapid expansion of coastal aquaculture ponds in
622 China from Landsat observations during 1984–2016. Int. J. Appl. Earth Obs. 82, 101902.
623 https://doi.org/10.1016/j.jag.2019.101902
624 Romañacha, S.S., DeAngelis, D.L., Kohc, H.L., Li, Y.H., Teh, S.Y., Barizan, R.S.R., Zhai, L., 2018.
625 Conservation and restoration of mangroves: Global status, perspectives, and prognosis. Ocean
626 Coast. Manage. 154, 72–82. https://doi.org/10.1016/j.ocecoaman.2018.01.009
627 Song, Y.T., Chen, L.Y.,Kang, L.Y., Yang, G.B., Qin, S.Q., Zhang, Q.W., Mao, C., Kou, D., Fang, K.,
628 Feng, X.H., Yang, Y.H., 2021. Methanogenic community, CH_4 production potential and its
629 determinants in the active layer and permafrost deposits on the Tibetan Plateau. Environ. Sci.
630 Technol. 55, 11412-11423. https://doi.org/10.1021/acs.est.0c07267
631 Strack, M., Waddington, J.M., 2008. Spatiotemporal variability in peatland subsurface methane
632 dynamics. J. Geophys. Res.-Biogeo. 113, G02010. https://doi.org/10.1029/2007JG000472
633 Sun, Z.G., Sun, W.G., Tong, C., Zeng, C.S., Yu, X., Mou, X.J., 2015. China's coastal wetlands:
634 Conservation history, implementation efforts, existing issues and strategies for future
635 improvement. Environ. Int. 79, 25–41. http://dx.doi.org/10.1016/j.envint.2015.02.017
636 Tan, L.S., Ge, Z.M., Zhou, X.H., Li, S.H, Li, X.Z., Tang, J.W., 2020. Conversion of coastal wetlands,
637 riparian wetlands, and peatlands increases greenhouse gas emissions: A global meta-analysis.
638 Glob Change Biol. 26, 1638–1653. http://dx.doi.org/10.1111/gcb.14933
639 Tong, C., Morris, J.T., Huang, J.F., Xu, H., Wan, S.A., 2018. Changes in pore-water chemistry and
640 methane emission following the invasion of *Spartina alterniflora* into an oliogohaline marsh.
641 Limnol. Oceanogr. 63, 384–396. https://doi.org/10.1002/lno.10637
642 Tong, C., Wang, W.Q., Huang, J.F., Gauci, V., Zhang, L.H., Zeng, C.S., 2012. Invasive alien plants
643 increase CH_4 emissions from a subtropical tidal estuarine wetland. Biogeochemistry 111, 677–

693. https://doi.org/10.1007/s10533-012-9712-5

Tong C., Bastviken D., Tang K.W., Yang P., Yang H., Zhang Y.F., Guo Q.Q., Lai D.Y.F., 2021. Annual CO_2 and CH_4 fluxes in coastal earthen ponds with *Litopenaeus vannamei* in southeastern China. Aquaculture 545, 737229. https://doi.org/10.1016/j.aquaculture.2021.737229

Tong, C., She, C.X., Yang, P., Jin, Y.F., Huang, J.F., 2015. Weak correlation between methane production and abundance of methanogens across three brackish marsh zones in the Min River Estuary, China. Estuar. Coast. 38, 1872–1884. https://doi.org/10.1007/s12237-014-9930-2

Updegraff, K., Pastor, J., Bridgham, S.D., Johnston, C.A., 1995. Environmental and substrate controls over carbon and nitrogen mineralization in northern wetlands. Ecol. Appl. 5, 151–163. https://doi.org/10.2307/1942060

Vizza, C., West, W.E., Jones, S.E., Hart, J.A., Lamberti, G.A., 2017. Regulators of coastal wetland methane production and responses to simulated global change. Biogeosciences 14, 431–446. https://doi.org/10.5194/bg-14-431-2017

Wang, J., Yuan, J.J., Liu, D.Y., Xiang, J., Ding, W.X., Jiang, X.J., 2016. Research progresses on methanogenesis pathway and methanogens in coastal wetlands. Chinese Journal of Applied Ecology 27, 993-1001. https://doi.org/10.13287/j.1001-9332.201603.014

Wassmann, R., Neue, H.U., Bueno, C., Lantin, R.S., Alberto, M.C.R., Buendia, L.V., Bronson, K., Papen, H., Rennenberg, H., 1998. Methane production capacities of different rice soils derived from inherent and exogenous substrates. Plant Soil 203, 227–237.

Yang, P., Bastviken, D., Jin, B.S., Mou, X.J., Tong, C., 2017a. Effects of coastal marsh conversion to shrimp aquaculture ponds on CH_4 and N_2O emissions. Estuar. Coast. Shelf S. 199, 125–131. https://doi.org/10.1016/j.ecss.2017.09.023.

Yang, P., Lai, D.Y.F., Jin, B.S., Bastviken, D., Tan, L.S., Tong, C., 2017b. Dynamics of dissolved nutrients in the aquaculture shrimp ponds of the Min River estuary, China: Concentrations, fluxes and environmental loads. Sci. Total Environ. 603–604, 256–267. http://dx.doi.org/10.1016/j.scitotenv.2017.06.074

Yang, P., Yang, H., Lai, D.Y.F., Guo, Q.Q., Zhang, Y.F., Tong, C., Xu, C.B., Li, X.F., 2020a. Large contribution of non-aquaculture period fluxes to the annual N_2O emissions from aquaculture ponds in Southeast China. J. Hydrol. 582, 124550. https://doi.org/10.1016/j.jhydrol.2020.124550

Yang, P., Zhang, Y.F., Yang, H., Guo, Q.Q., Lai, D.Y.F., Zhao, G.H., Li, L. Tong, C., 2020b.

674 Ebullition was a major pathway of methane emissions from the aquaculture ponds in southeast
675 China. Water Res. 184, 116176. https://doi.org/10.1016/j.watres.2020.116176
676 Yang, P., Zhang, Y., Yang, H., Zhang, Y.F., Xu, J., Tan, L.S., Tong, C., Lai, D.Y.F., 2019a. Large fine-
677 scale spatiotemporal variations of CH_4 diffusive fluxes from shrimp aquaculture ponds affected
678 by organic matter supply and aeration in Southeast China. J. Geophys. Res.-Biogeo. 124, 1290–
679 1307. https://doi.org/10.1029/2019JG005025
680 Yang, P., Wang, M.H., Lai, D.Y.F., Chun, K.P., Huang, J.F., Wan, S.A., Bastviken, D., Tong, C., 2019b.
681 Methane dynamics in an estuarine brackish *Cyperus malaccensis* marsh: Production and
682 porewater concentration in soils, and net emissions to the atmosphere over five years. Geoderma
683 337, 132–142. https://doi.org/10.1016/j.geoderma.2018.09.019
684 Yang, P., Zhao, G.H., Tong, C., Tang, K.W., Lai, D.Y.F., Li, L., Tang, C., 2021. Assessing nutrient
685 budgets and environmental impacts of coastal land-based aquaculture system in southeastern
686 China. Agr. Ecosyst. Environ. 322, 107662. https://doi.org/10.1016/j.agee.2021.107662
687 Yang, Y.Y., Chen, J.F., Tong, T.L., Xie, S.G., Liu, Y., 2020. Influences of eutrophication on
688 methanogenesis pathways and methanogenic microbial community structures in freshwater lakes.
689 Environ. Pollut. 260, 114106. https://doi.org/10.1016/j.envpol.2020.114106
690 Ye, F., Hu, C.C., Wang, Y., Wu, J.P., Hong, Y.G., 2021. Biogeographic pattern of methanogenic
691 community in surface water along the Yangtze River. Geomicrobiol. J. 38, 588–597.
692 https://doi.org/10.1080/01490451.2021.1905113
693 Yuan, J.J., Xiang, J., Liu, D.Y., Kang, H., He, T.H., Kim, S., Lin, Y.X., Freeman, C., Ding, W.X.,
694 2019a. Rapid growth in greenhouse gas emissions from the adoption of industrial-scale
695 aquaculture. Nat. Clim. Change 9 (4), 318–322. https://doi.org/10.1038/s41558-019-0425-9
696 Yuan, J.J., Liu, D.Y., Ji, Y., Xiang, J., Lin, Y.X., Wu, M., Ding, W.X., 2019b. *Spartina alterniflora*
697 invasion drastically increases methane production potential by shifting methanogenesis from
698 hydrogenotrophic to methylotrophic pathway in a coastal marsh. J. Ecol. 107, 2436–2450.
699 https://doi.org/10.1111/1365-2745.13164
700 Zogg, G.P., Zak, D.R., Ringelberg, D.B., White, D.C., MacDonald, N.W., Pregitzer, K.S., 1997.
701 Compositional and functional shifts in microbial communities due to soil warming. Soil Soil Sci.
702 Soc. Am. J. 61, 475–481. https://doi.org/10.2136/sssaj1997.03615995006100020 0
703 Zhou, C.Q., Peng, Y., Yu, M.T., Deng, Y., Chen, L., Zhang, L.Q., Xu, X.G., Zhang, S.Y., Y, Yan., Wang,

G.X., 2022. Severe cyanobacteria accumulation potentially induces methylotrophic methane producing pathway in eutrophic lakes. Environ. Pollut. 292(Part B), 118443. https://doi.org/10.1016/j.envpol.2021.118443

Zhou, H., Gao, Y., Jia, X.H., Wang, M.M., Ding, J.J., Cheng, L., Bao, F., Wu, B., 2020. Network analysis reveals the strengthening of microbial interaction in biological soil crust development in the Mu Us Sandy Land, northwestern China. Soil Biol. Biochem. 144, 107782. https://doi.org/10.1016/j.soilbio.2020.107782

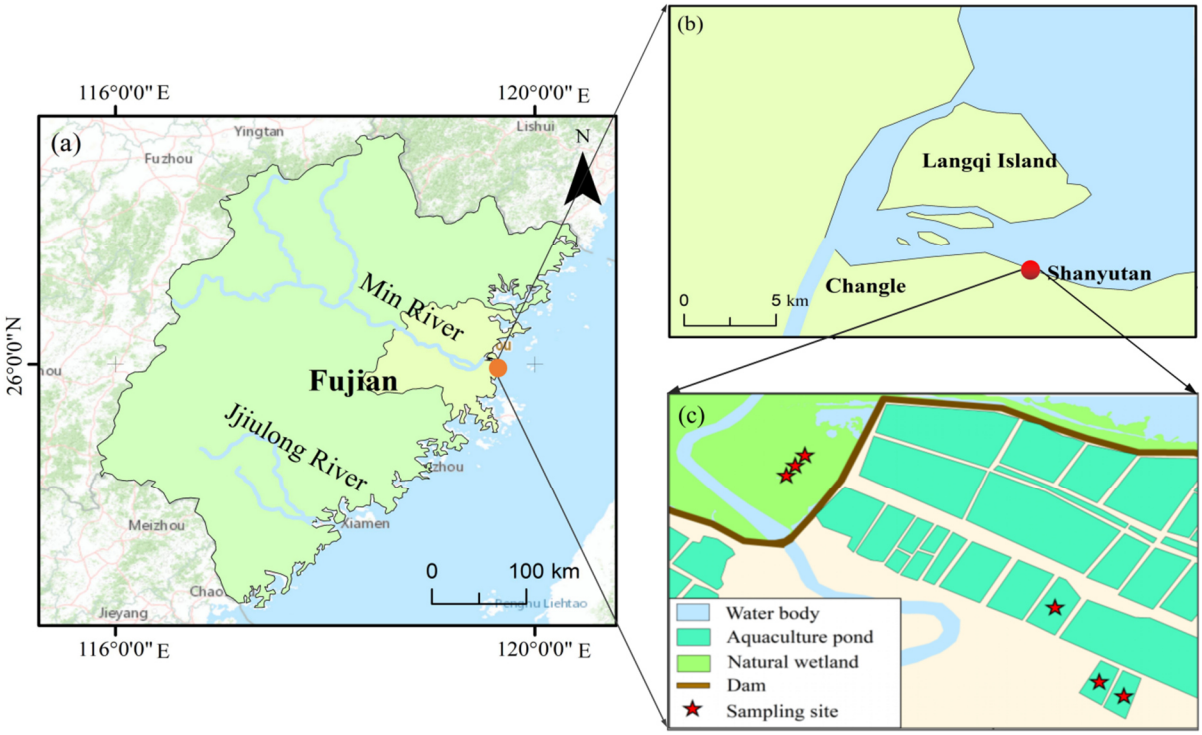

Fig. 1. Location of the brackish *Cyperus malaccensis* marsh and adjacent aquaculture shrimp ponds in the Min River Estuary, southeastern China.

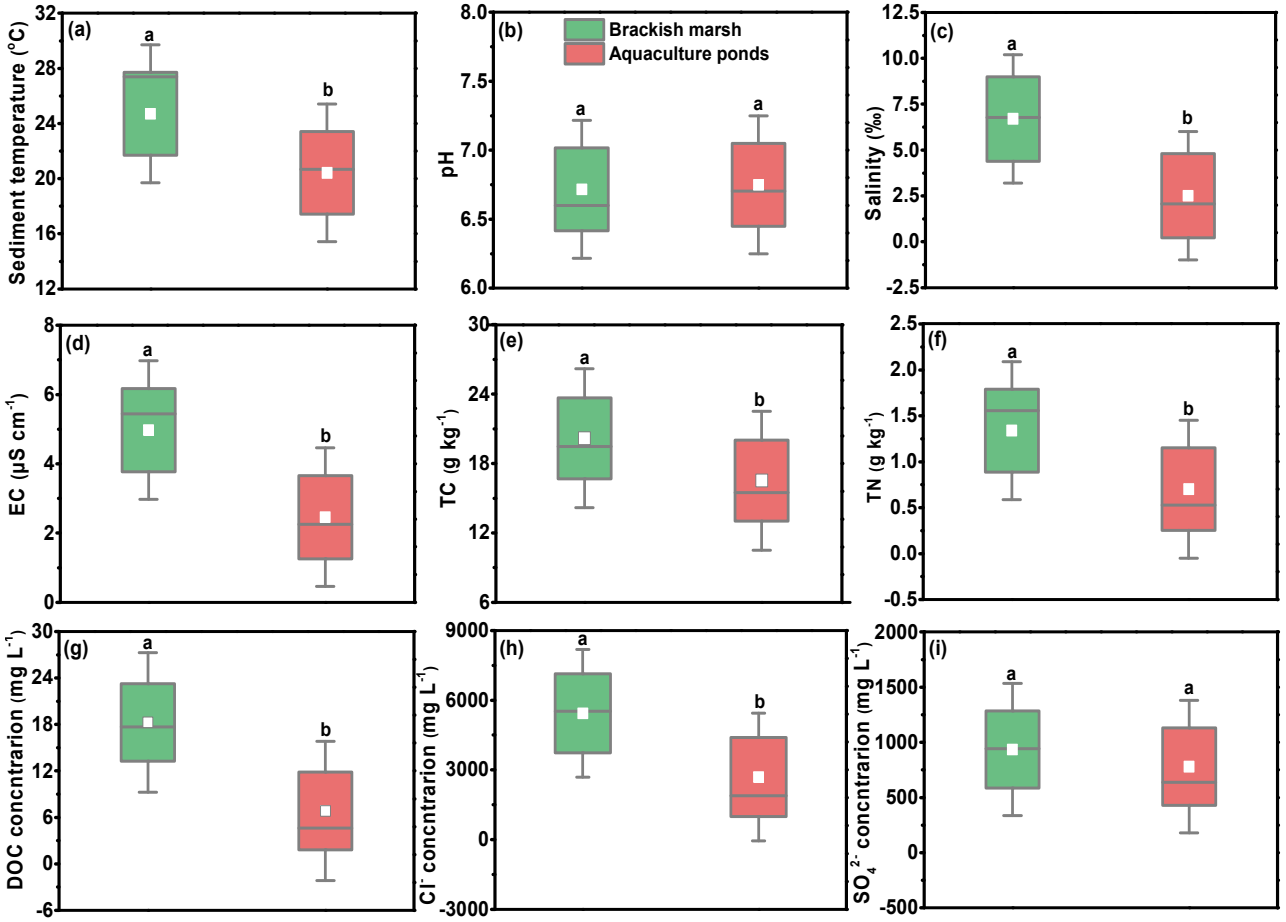

Fig. 2. Boxplots of physicochemical parameters of sediment and porewater from the brackish marshes and the aquaculture ponds. Each box shows the quartiles and median, while the square and whiskers represent the mean and values within 1.5 times of the interquartile range, respectively. Different lowercase letters within each panel indicate significant differences at the $p<0.05$ level between the brackish marsh ($n = 30$) and the aquaculture ponds ($n = 90$).

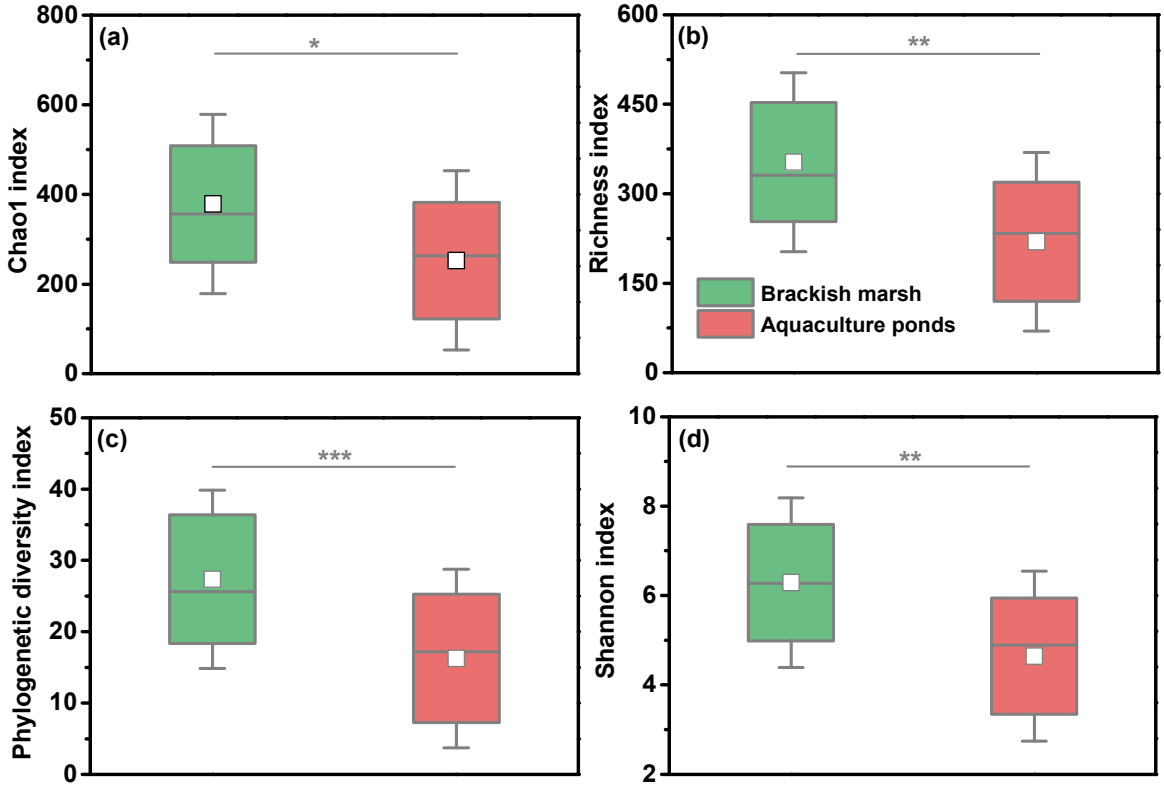

Fig. 3. Boxplots of Alpha diversity indices (i.e., Chao1 (a), Richness (b), Phylogenetic diversity (c), and Shannon (d)) of the sediment methanogenic archaea communities in the brackish marsh and the aquaculture ponds. The symbols *, ** and *** indicate significant differences at the 0.05, 0.01 and 0.001 levels, respectively.

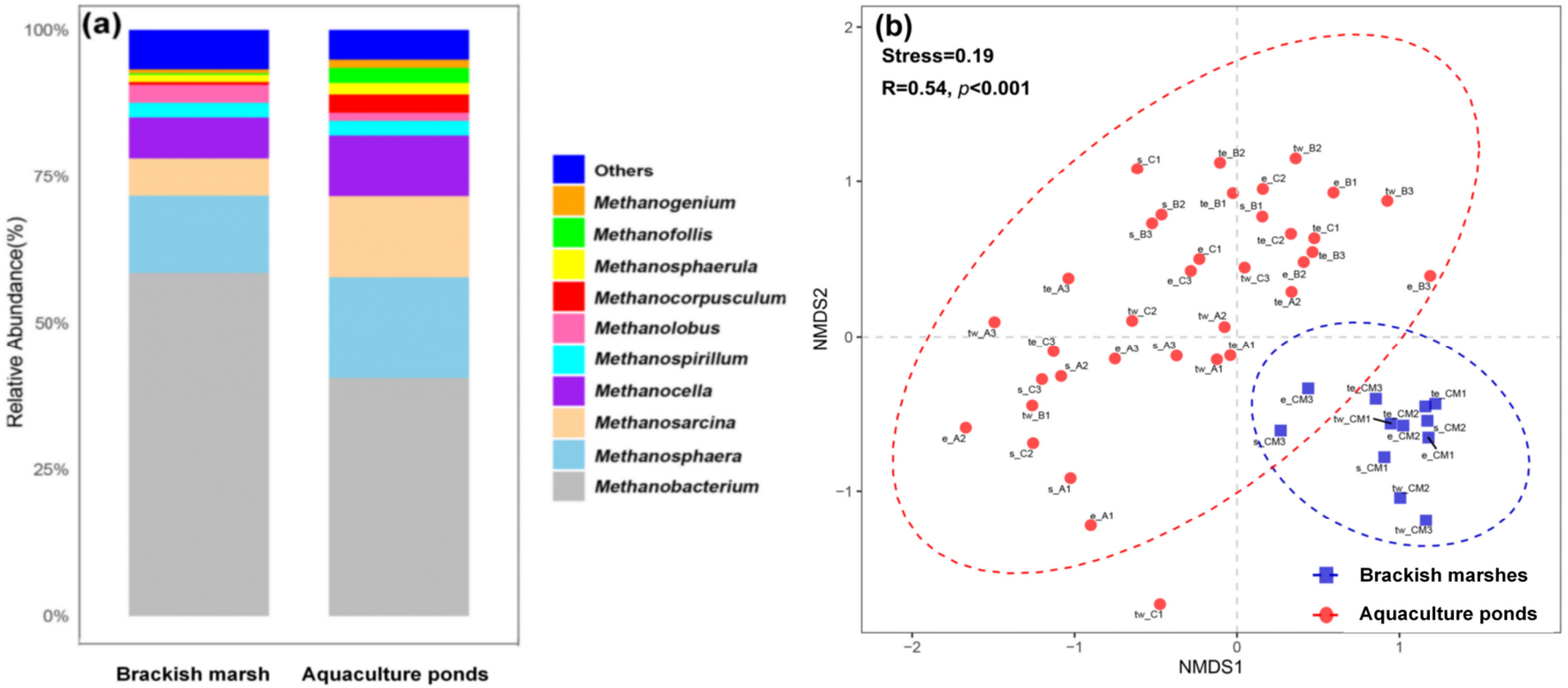

Fig. 4. Compositions of sediment methanogenic archaea communities (a) and nonmetric multidimensional scaling (NMDS) analysis of the Bray-Curtis distance matrix for the sediment methanogenic archaea communities in the two habitats (b). The indicated ANOSIM R statistics and PerMANOVA P values for brackish marsh and aquaculture ponds are based on comparisons among sampling sites.

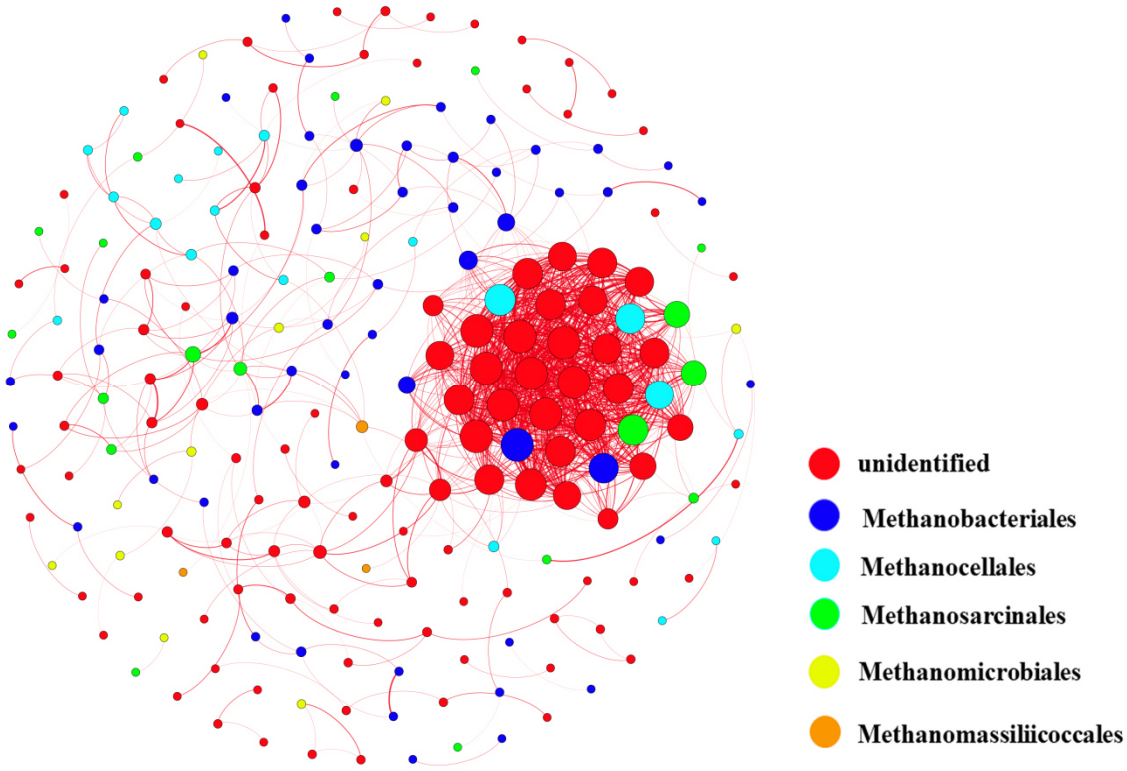

Fig. 5. Methanogenic archaea co-occurrence networks in the brackish marshes and the aquaculture ponds based on correlation analysis. The size of the node is proportional to the number of connections.

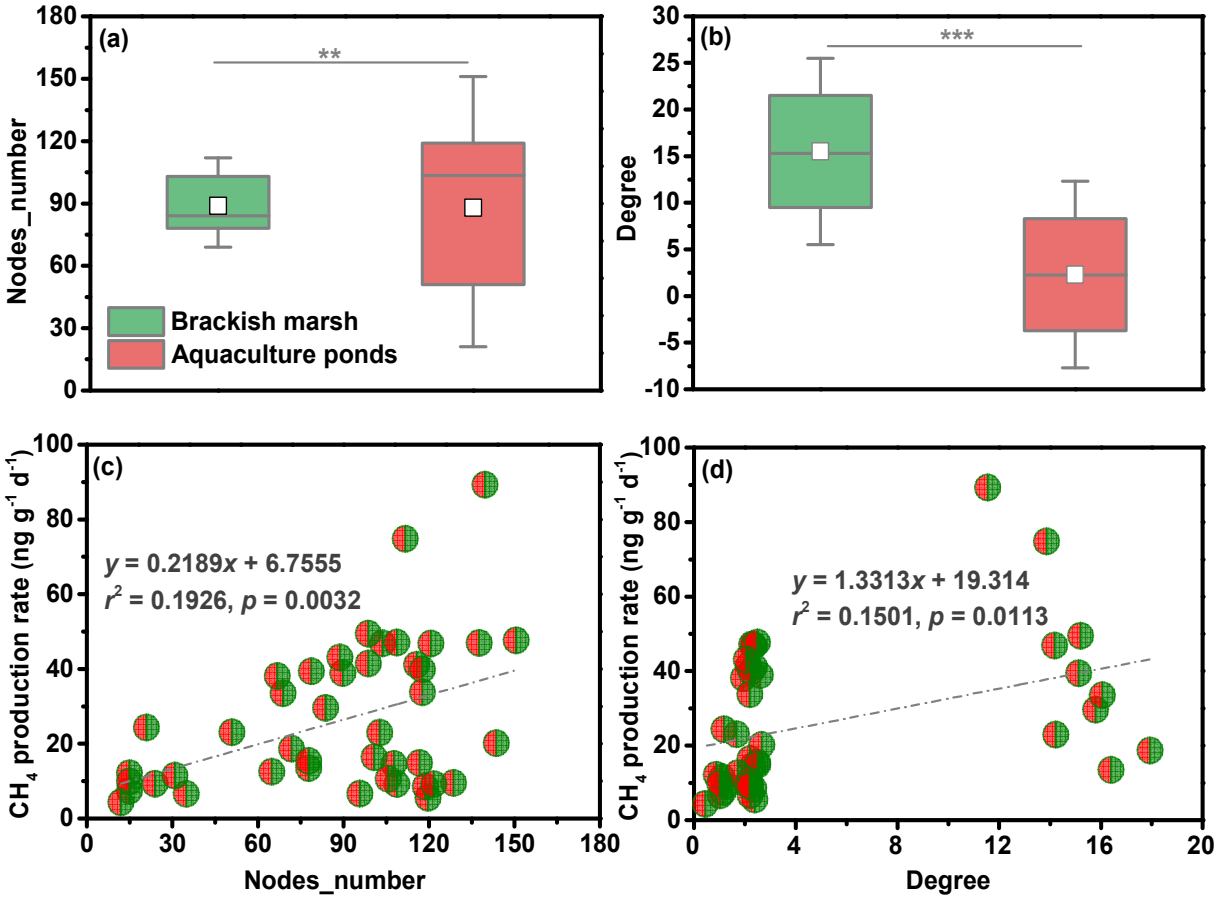

Fig. 6. Comparison of microbial network complexity between the two habitats in terms of node numbers (a) and degree (b), and correlations between sediment CH_4 production potential and sediment methanogenic archaea network topological features in terms of node numbers (c) and degree (d) across all samples.

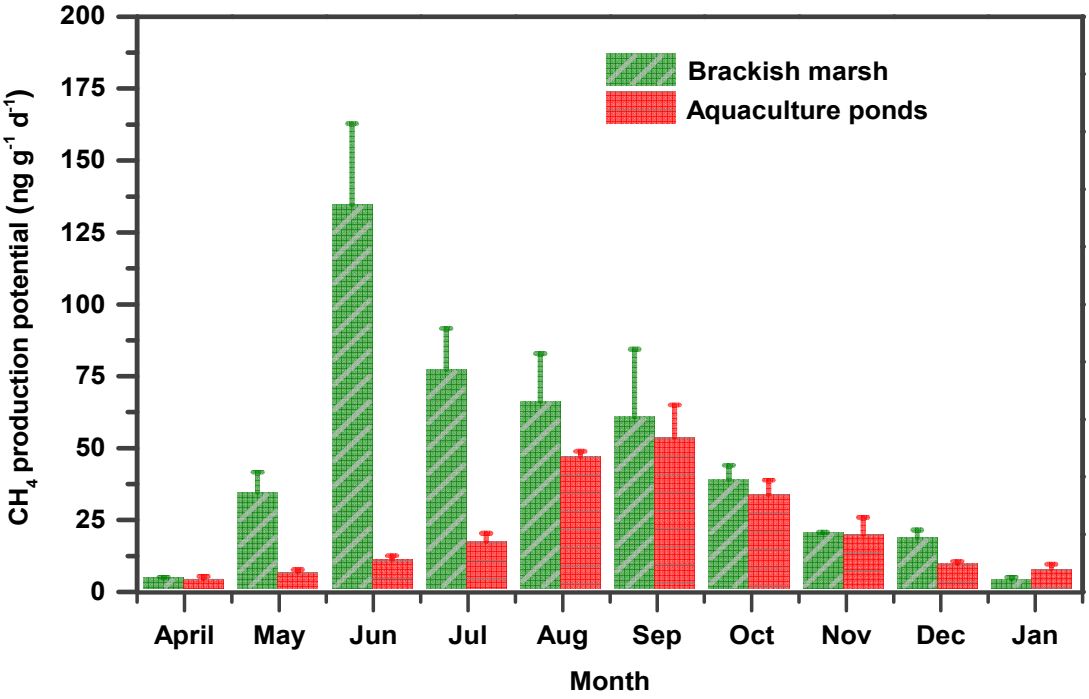

Fig. 7. Monthly sediment CH_4 production potential in the brackish marsh and the aquaculture ponds. Bars represent mean ± SE (n = 3).

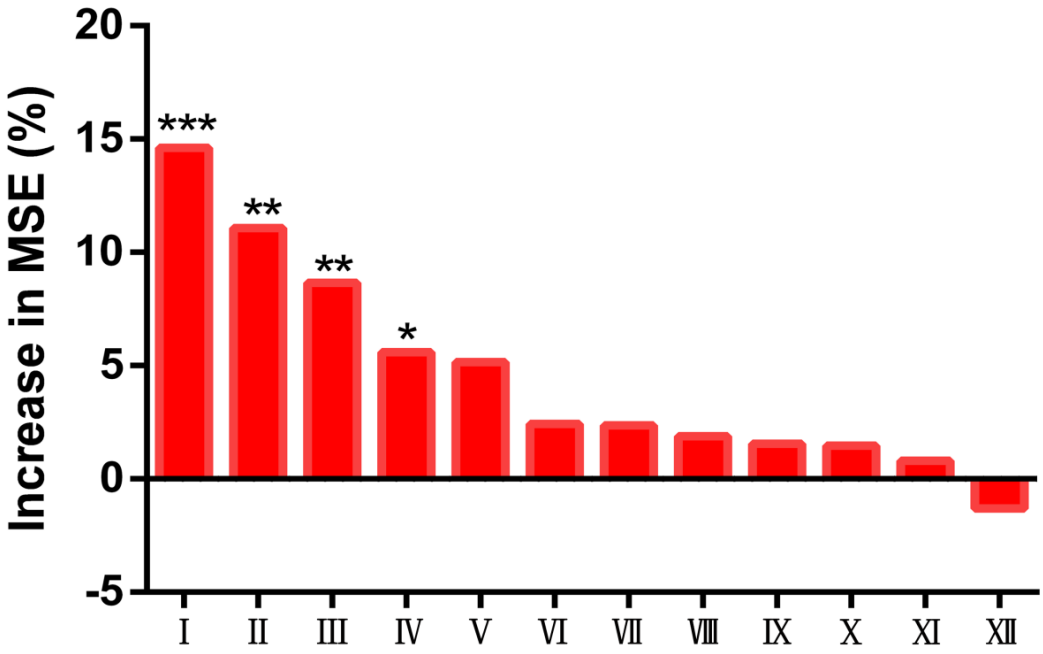

Fig. 8. Predictive power of different parameters, expressed as increase in mean squared error (MSE; %), for sediment CH_4 production potential based on Random Forest Analysis (RFA). The symbols *, ** and *** above the bars indicate a significant effect of the parameter at the 0.05, 0.01 and 0.001 levels, respectively. **I:** total carbon (TC); **II:** porewater SO_4^{2-} concentration; **III:** sediment temperature (T_S); **IV:** richness index; **V:** porewater Cl^- concentration; **VI:** Shannon index; **VII:** porewater DOC concentration; **VIII:** sediment salinity; **IX:** total nitrogen (TN); **X:** sediment pH; **XI:** electrical conductivity (EC); **XII:** phylogenetic diversity index.

Table 1 Pearson correlation coefficients between sediment CH_4 production potential and different environmental variables in the brackish marsh and the aquaculture ponds. Significant correlations are denoted by the symbols * ($p < 0.05$) and ** ($p < 0.01$); NS means non-significant relationship.

Environmental variables	**Sediment CH_4 production potential**		
	Brackish marsh	Aquaculture ponds	All data
Sediment			
Temperature (T_S)	0.500**	0.838**	0.603**
pH	NS	NS	NS
Salinity	-0.744**	-0.699**	-0.360**
Electrical conductivity (EC)	-0.700**	-0.579**	-0.392**
Total carbon (TC)	0.755**	0.921**	0.776**
Total nitrogen (TN)	0.454*	NS	0.365**
Porewater			
DOC concentration	0.675**	0.814**	0.602**
Cl^- concentration	-0.628**	-0.586**	-0.416**
SO_4^{2-} concentration	-0.631**	-0.669**	-0.535**

Supporting Information

Changes in sediment methanogenic archaea community structure and methane production potential following conversion of coastal marsh to aquaculture ponds

Ping Yang[a,b,c*], Kam W. Tang[d], Chuan Tong[a,b,c], Derrick Y. F. Lai[e], Lianzuan Wu[b], Hong Yang[f,g], Linhai Zhang[a,b,c], Chen Tang[b], Yan Hong[b], Guanghui Zhao[b]

[a]*School of Geographical Sciences, Fujian Normal University, Fuzhou 350007, P.R. China*

[b]*Key Laboratory of Humid Subtropical Eco-geographical Process of Ministry of Education, Fujian Normal University, Fuzhou 350007, P.R. China*

[c]*Research Centre of Wetlands in Subtropical Region, Fujian Normal University, Fuzhou 350007, P.R. China*

[d]*Department of Biosciences, Swansea University, Swansea SA2 8PP, U. K.*

[e]*Department of Geography and Resource Management, The Chinese University of Hong Kong, Hong Kong, China*

[f]*College of Environmental Science and Engineering, Fujian Normal University, Fuzhou, 350007, China*

[g]*Department of Geography and Environmental Science, University of Reading, Reading, UK*

***Correspondence to:** Ping Yang (yangping528@sina.cn)

Telephone: 086-0591-87445659 **Fax:** 086-0591-83465397

Supporting Information Summary

No. of pages: 6 No. of figures: 3 No. of tables: 0

Page S3: Figure S1. Seasonal values of sediment temperature (T_S), pH, salinity, conductivity (EC), total carbon (TC), total nitrogen (TN), porewater DOC concentration, Cl^- concentration and SO_4^{2-} concentration in the brackish marsh and the aquaculture ponds during the study period

Page S4: Figure S2. Seasonal sediment CH_4 production potential in the brackish marsh and the aquaculture ponds during the study period.

Page S5: Figure S3 Relationships between sediment CH_4 production potential and the alpha diversity (i.e., Chao1 (a), Richness (b), Phylogenetic diversity (c), and Shannon (d)) of sediment methanogenic archaea communities across the two habitats.

Page S6: Figure S4. Precipitation record for the Min River Estuary from March 2019 to April 2020.

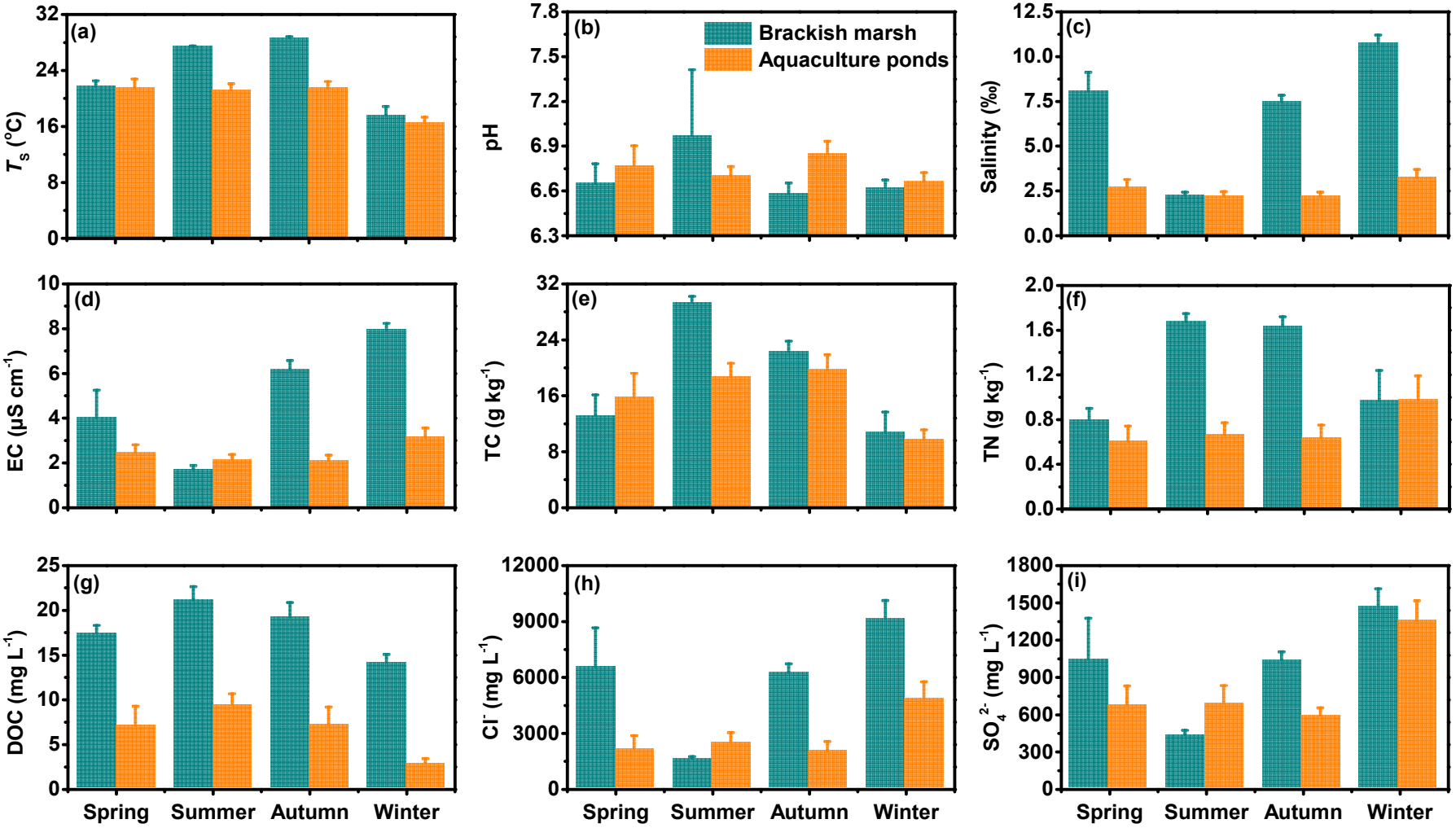

Figure S1 Seasonal values of sediment temperature (T_S), pH, salinity, conductivity (EC), total carbon (TC), total nitrogen (TN), porewater DOC concentration, Cl^- concentration and SO_4^{2-} concentration in the brackish marsh and the aquaculture ponds during the study period.

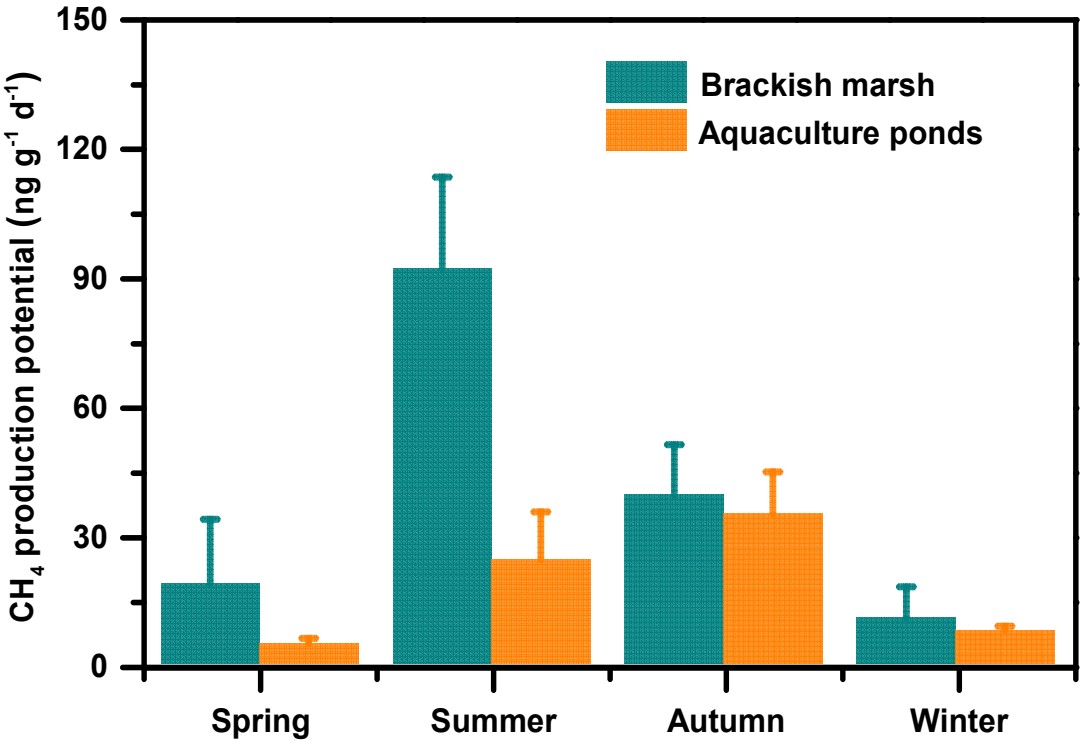

Figure S2 Seasonal sediment CH_4 production potential in the brackish marsh and the aquaculture ponds during the study period.

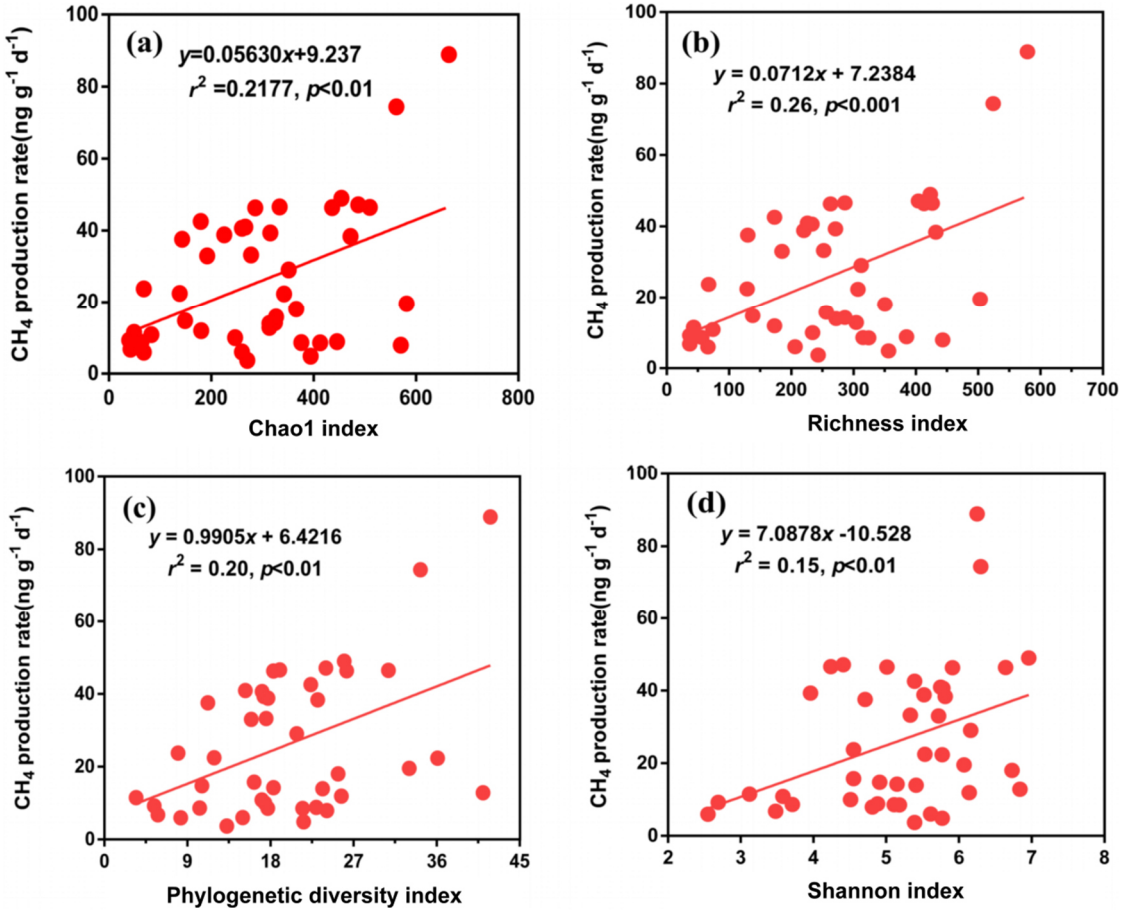

Figure S3 Relationships between sediment CH_4 production potential and the alpha diversity indices (i.e., Chao1 (a), Richness (b), Phylogenetic diversity (c), and Shannon (d)) of sediment methanogenic archaea communities across the two habitats.

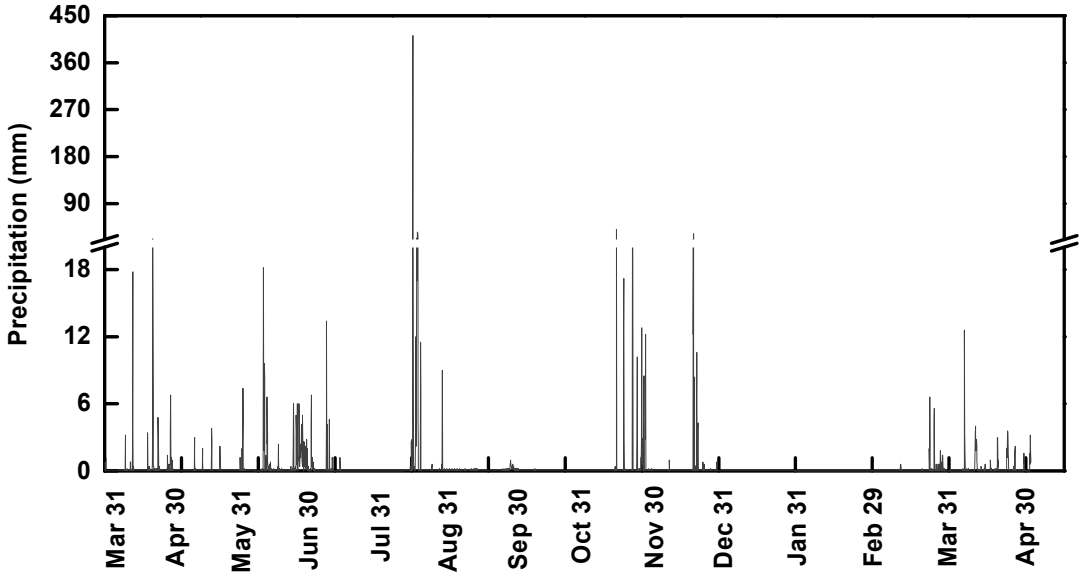

Figure S4 Precipitation record for the Min River Estuary from March 2019 to April 2020. [Precipitation were measured by the automatic weather station at the Min River Estuary Ecological Station in the Shanyutan Wetland.]